JACS
JOURNAL OF THE AMERICAN CHEMICAL SOCIETY

Article

pubs.acs.org/JACS

Visualization of RNA-Quadruplexes in Live Cells

Aurélien Laguerre,[†] Kyle Hukezalie,[‡] Pascale Winckler,[§] Fares Katranji,[†] Gaëtan Chanteloup,[†] Marc Pirrotta,[†] Jean-Marie Perrier-Cornet,[§] Judy M. Y. Wong,*[,‡] and David Monchaud*[,†]

[†]Institute of Molecular Chemistry, University of Dijon, ICMUB CNRS, UMR6302 Dijon, France

[‡]Faculty of Pharmaceutical Sciences, University of British Columbia, Vancouver, BC V6T 1Z3, Canada

[§]Dimacell Imaging Ressource Center, UMR PAM, University of Burgundy, Agrosup, 21000 Dijon, France

Supporting Information

ABSTRACT: Visualization of DNA and RNA quadruplex formation in human cells was demonstrated recently with different quadruplex-specific antibodies. Despite the significant interest in these immunodetection approaches, dynamic detection of quadruplex in live cells remains elusive. Here, we report on NaphthoTASQ (N-TASQ), a next-generation quadruplex ligand that acts as a multiphoton turn-on fluorescent probe. Single-step incubation of human and mouse cells with N-TASQ enables the direct detection of RNA-quadruplexes in untreated cells (no fixation, permeabilization or mounting steps), thus offering a unique, unbiased visualization of quadruplexes in live cells.

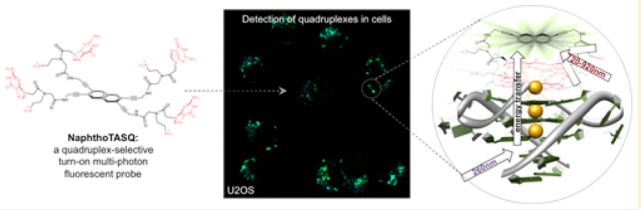

INTRODUCTION

The diversity of cellular processes in which G-quadruplexes are thought to play key regulatory roles (including chromatin remodeling, regulation of gene expression, DNA-damage repair, etc.)[1] is offset by the paucity of their demonstrable existence in cells. Quadruplexes are non-B DNA/RNA structures arising from the assembly of four G-rich strands held together through guanine associations in G-quartets, which are planar and cyclic arrays of four guanine residues connected via eight Hoogsteen hydrogen bonds.[2] Biologically relevant quadruplex-forming sequences comprise four G-stretches separated by intervening sequences of various length and composition, poised to self-assemble into quadruplexes with great topological plasticity[3] when transiently relieved from their duplex constraint. The location and evolutionary conserved nature of repetitive G-rich sequences strongly suggests that quadruplexes may indeed harbor critical genomic functions.[4] However, the significance of their regulatory roles are often confounded by their contribution to both positive and negative cellular outcomes (depending on their location, they can trigger genetic instability[5] or provide genomic protection),[6] coupled with the aforementioned scarcity of compelling evidence of their actual existence in a cellular context.

Chemists and biologists have joined efforts to create molecular tools to assess the actual relevance of quadruplexes in cells. To date, the strongest arguments have been provided by quadruplex-specific antibodies,[7−9] including BG4[8] and 1H6.[9] However, an important limitation of immunodetection is its restriction to fixed and permeabilized cells (to allow entry of cell-impermeable antibodies), therefore limiting the detection of quadruplexes to cells whose morphological integrity is impaired. Rodriguez et al. reported on an elegant way to tackle this issue, performing cell-based chemical labeling of a quadruplex ligand (PDS-α) bound to its genomic targets prior to cell fixing, thus enabling the identification of quadruplexes in functioning cells.[10] However, subsequent chemical manipulations, including an *in situ* click-chemistry step to conjugate PDS-α to the AlexaFluor reporter, again necessitate cell fixation. With this in mind, and inspired by the wealth of knowledge now available on the design and use of quadruplex-selective fluorescent probes,[11] we devised a strategy based on the use of binding-activated fluorescent quadruplex ligands that allow for the detection of quadruplexes with a direct labeling protocol. Our method requires neither postfixation chemical labeling steps (PDS-α), nor multistep/reagent cascades (BG4 or 1H6). To this end, we studied NaphthoTASQ (aka N-TASQ, Figure 1), a new biomimetic quadruplex ligand that is both a smart ligand and a smart probe. In line with the pioneering works carried out with carbazole derivatives,[12] our approach allows for the direct visualization of quadruplexes in cells via multiphoton microscopy techniques. Our findings offer an unbiased detection of RNA quadruplexes in live cells.

EXPERIMENTAL SECTION

Full experimental details for the syntheses, purifications and characterizations of N-TASQ are given in the Supporting Information. Protocols for the preparation of the oligonucleotides, for FRET-melting, UV−vis, and fluorescence experiments as well as cellular images carried out with fixed cells are also described in Supporting Information.

Cell Culture. MCF7, B16F10, and U2OS cells were routinely cultured in 75 cm^2 tissue culture flasks (Corning) at 37 °C in a humidified, 5% CO_2 atmosphere in DMEM (MCF7 and U2OS) or RPMI (B16F10) supplemented with 10% fetal bovine serum (FBS) and 100 U penicillin−streptomycin mixture (1.0 U·mL^{-1} Pen/1.0 mg·mL^{-1}

Received: April 7, 2015
Published: June 9, 2015

DOI: 10.1021/jacs.5b03413
J. Am. Chem. Soc. 2015, 137, 8521−8525

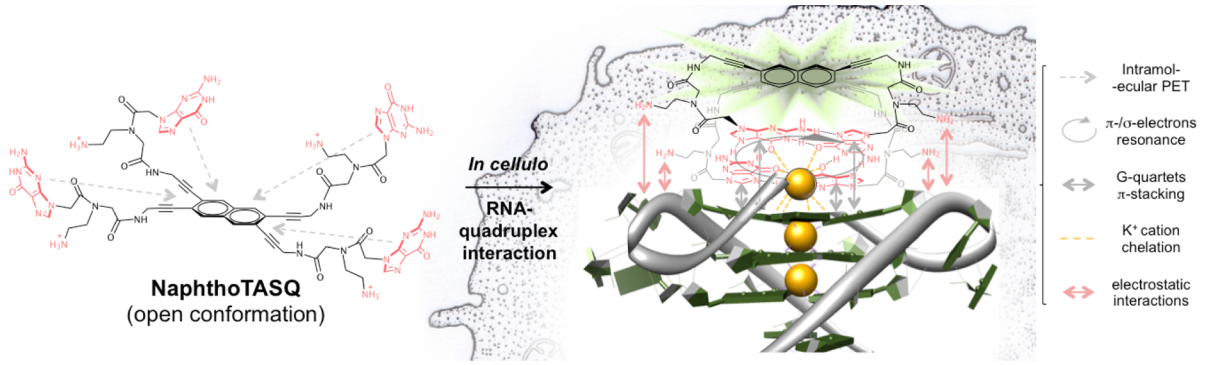

Figure 1. Chemical structure of NaphthoTASQ (N-TASQ) and schematic representation of its open (left, its fluorescence is quenched via intramolecular photoinduced electron transfer, dashed gray arrows) and closed conformations (right, promoted by quartet self-association (gray arrows), cation chelation (yellow dashed lines) and electrostatic interactions (pink arrows)). The formation of the intramolecular quartet relieves the template from its electronic restraint, causing its fluorescence to be restored.

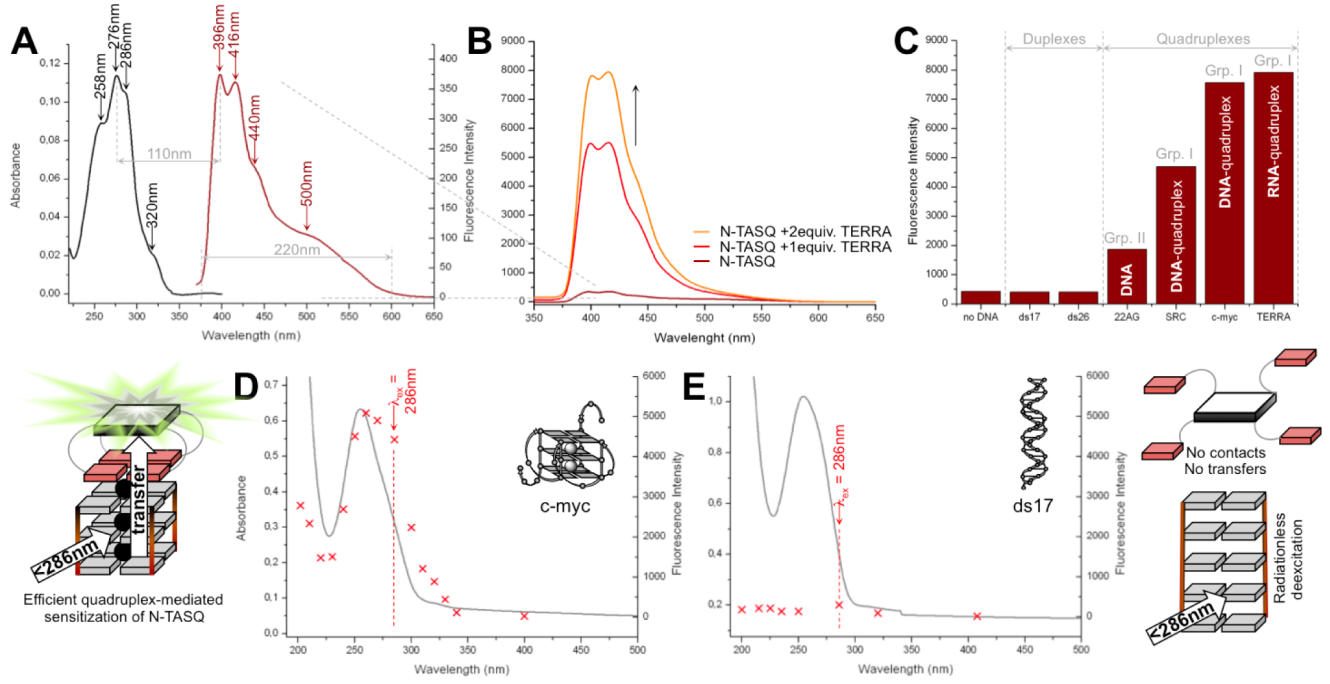

Figure 2. Photophysical properties of N-TASQ *in vitro*: (A) UV–vis (dark line) and fluorescent spectra (brown line, λ_{ex} = 286 nm) of N-TASQ (2 μM) in water. (B) Fluorescent spectra of N-TASQ (2 μM) before (brown line) and after addition of 1 and 2 molar equiv of the RNA quadruplex TERRA (red and orange lines, respectively). (C) Results of the fluorescence studies (λ_{ex} = 286 nm, λ_{em} = 396 nm) carried out with N-TASQ (2 μM), alone ("no DNA" bar) or in presence (4 μM) of DNA duplexes (ds17 and ds26), DNA quadruplexes (22AG, SRC and c-myc), and RNA quadruplex (TERRA). (D and E) Nucleic acid-mediated sensitization of N-TASQ: overlap of the UV–vis spectra (gray lines) of a 1:1 N-TASQ/quadruplex complex (2 μM) and fluorescence maxima (red stars) recorded as a function of λ_{ex} for experiments carried out with c-myc (D) or ds17 (E). Experiments involving DNA/RNA were done in 10 mM lithium cacodylate buffer (pH 7.2) and 90 mM LiCl/10 mM KCl.

Strep, Corning). Cells were subcultured twice weekly using standard protocols: removal of the medium, PBS washing step, incubation with Trypsin–EDTA (0.25%, Corning) 5 min at 37 °C; cells were subsequently manually harvested, counted with a Coulter Counter (Beckman Coulter), and reseeded in appropriate density.

Live-Cell Imaging. For N-TASQ live-culture incubation experiments, cells were seeded onto round glass coverslips in 8-well plates (Corning), allowed to recover for 24 h, and then treated with TASQ (5 μM) for 48 h. After incubation, cells were washed 3× with PBS, and images were collected (in PBS) on a Nikon A1-MP scanning microscope using a 720 nm excitation (IR laser Chameleon, Coherent). Imaging was carried out with a 60× Apo LWD objective (NA: 1.27, Water Immersion, Nikon, Japan). Fluorescence emission was collected on three detection channels (FF01–492/SP "DAPI channel", FF03–525/50 "FITC channel", and FF01–629/56 "Alexa channel", Semrock).

RESULTS AND DISCUSSION

We recently reported on a series of biomimetic ligands that elicit remarkable affinity and selectivity for quadruplexes, being structurally dynamic and adopting quadruplex-binding conformation only upon interaction with their nucleic acid targets. Synthetic G-quartets (SQ) provide the structural basis of these new-generation ligands. Their unique properties make them the first biomimetic ligands, with SQ that interact with native G-quartets according to a bioinspired "*like-likes-like*" association,[13] smart quadruplex ligands, with SQ that actively assemble only in the presence of their native G-quartet targets,[14] and twice-as-smart quadruplex ligands, with SQ that are both smart quadruplex ligands and smart fluorescent probes.[15] The first prototype of twice-as-smart quadruplex ligands, named

DOI: 10.1021/jacs.5b03413
J. Am. Chem. Soc. 2015, 137, 8521–8525

PyroTASQ, has proved to be an efficient quadruplex-specific probe for *in vitro* investigations, enabling multicolor identification of quadruplexes via EMSA experiments.[15] However, our attempts to use PyroTASQ for cellular imaging were partly successful only (see the Supporting Information), due to its propensity to aggregate in extracellular space. Here, we report on a new twice-as-smart ligand, named N-TASQ (Figure 1), which was specifically designed for cellular investigations. The pyrene of PyroTASQ was replaced by a naphthalene template with the intent to (i) decrease its capacity to form aggregates, (ii) improve its water-solubility, and (iii) blue-shift its absorbance properties below 300 nm. This hypsochromic shift brings double dividend, enabling it to overlap nucleic acid absorbance (using them as sensitizers via energy transfer) and to absorb more than one photon at a time upon laser excitation in the near-infrared window (>600 nm). N-TASQ thus conceptually differs from PyroTASQ in that its sensitization is multiphoton and both direct and DNA-mediated: N-TASQ thus behaves as a cell-compatible molecular sensor that fits only into quadruplex fixtures, using them as structure-specific sensitizing antennas.

The synthesis of N-TASQ, detailed in Supporting Information, is based on a quadruple Sonogashira-Heck-Cassar coupling reaction.[16] We first prepared the 3,6-dibromo-2,7-bis-(trifluoromethanesulfonyl)-naphthalene according to a reported three-step protocol from commercially available 2,7-dihydroxynaphthalene.[17] This precursor was coupled with *N*-Boc-propargylamine, which consequently reacted with two aryl-bromide and two aryl-triflate moieties. After a *N*-Boc-deprotection step, the resulting compound reacted with PNA guanine monomers[16] to provide, after a final deprotection step, pure N-TASQ after flash chromatography.

The DNA/RNA quadruplex binding properties of N-TASQ were first assessed *in vitro* via a series of fluorescence FRET-melting assays (see Supporting Information, Figures S4−S7).[18] Experiments were implemented against a panel of biologically relevant doubly labeled oligonucleotides, including three DNA quadruplexes (i.e., F21T, F-myc-T and F-kit-T),[19] three RNA quadruplexes (i.e., L-TERRA, L-TRF2 and L-VEGF),[20] along with one duplex-DNA as control. We also performed competitive FRET-melting experiments carried out with both F21T and L-TERRA in the presence of an excess of unlabeled duplex (ds26), quadruplex-DNA (TG5T), and quadruplex-RNA (UG5U) high-stability competitors.[14] Collectively, results detailed in Supporting Information indicate that N-TASQ is an excellent quadruplex ligand, with high affinity for quadruplexes (with $\Delta T_{1/2}$ values between 12.3 and 12.5 °C and 11.0−17.4 °C for DNA and RNA quadruplexes, respectively, at 1 μM ligand concentration, Supporting Information Figures S4−S7) and remarkable selectivity over duplexes (with ^{FRET}S >0.89 in the presence of 50 molar equiv of ds26, Supporting Information Figures S4−S7).

Given that N-TASQ is a promising ligand, its spectroscopic properties (alone or in the presence of nucleic acids) were subsequently mapped *in vitro*. Absorbance spectrum of N-TASQ displays three vibronic bands, centered on 258, 276, and 286 nm (ε = 44 500, 56 900, and 52 600 $M^{-1}\cdot cm^{-1}$, plus a shoulder at 320 nm, Figure 2A), thereby fully overlapping nucleic acid absorbance. We believe that this latter point, usually considered as a drawback (shielding), could help amplify the N-TASQ fluorescence, due to the antenna role that nucleic acids can play upon UV irradiation (below 310 nm), to sensitize bound dyes via energy transfer,[21] known to be particularly favored with quadruplexes.[22] Our strategy thus deviates from classical approaches since our ligand is a light-up probe whose fluorescence is triggered by structure-specific DNA/RNA binding. Additionally, the absorbance properties of quadruplex-bound N-TASQ make multiphoton absorption possible in the NIR window (>600 nm). The fluorescence of N-TASQ in the absence of quadruplex-binding is weak (excitation at 286 nm, Figure 2A), as expected for a light-up probe.[11] As previously demonstrated with ^{PNA}DOTASQ and PyroTASQ,[14,15] N-TASQ is in its open conformation when free in solution, the fluorescence of its naphthalene template is quenched by the four surrounding guanines via intramolecular photoinduced electron transfer (Figure 1).[21] N-TASQ fluorescence spectrum exhibits two maxima at 396 and 416 nm (plus shoulders near 440 and 500 nm), thus giving a notable Stokes shift (>110 nm), presumably due to efficient vibronic couplings, and a wide fluorescence signal (380−600 nm), making N-TASQ suitable for detection via emission filters routinely employed during cellular imaging (vide infra).

Upon addition of nucleic acids *in vitro*, the fluorescence of N-TASQ is enhanced (up to 22-fold) in a structure-specific manner, in agreement with its light-up nature. Upon interaction with quadruplexes, N-TASQ folds into its closed conformation and the formation of the intramolecular G-quartet leads to a redistribution of the guanine electrons onto the four guanines (Figure 1). This resonance contributes to the stability of the quartet (along with Hoogsteen H-bonds), relieves the template from its electronic restraint and restores its fluorescence.[15,23] As an example, the addition of 2 molar equiv of RNA quadruplex TERRA triggers a 22-fold improvement of N-TASQ fluorescence (excitation at 286 nm, Figure 2C, and Supporting Information Figure S8). Similar titration experiments were performed with two duplexes (ds17 and ds26), three DNA quadruplexes belonging to two different topological groups[24] (group I, c-myc and SRC; and group II, 22AG) and one RNA quadruplex (TERRA). Collected results show that N-TASQ behaves similarly to PyroTASQ, labeling quadruplexes with accessible external G-quartets (group I: TERRA, c-myc and SRC) more efficiently than looped quadruplexes (22AG, due to lower accessibility of the binding site and the presence of loop nucleobases that might attenuate template fluorescence through intermolecular energy transfer).[15] Notably, N-TASQ does not label duplexes (ds17 and ds26), confirming its utility as a specific probe for *in vitro* investigations of quadruplex structures.

With one-photon absorption experiments of quadruplex/N-TASQ complexes, using excitation wavelengths where DNA/RNA absorbance occurs, we verified that nucleic acids could act as structure-specific N-TASQ sensitizer. The straightforward relationship between the absorbance of the quadruplex/ligand assembly (Figure 2D, gray line, Supporting Information Figure S9) and the N-TASQ fluorescence signals collected upon excitation at different wavelengths along that UV−vis spectrum (red stars) strongly advocates for an efficient energy transfer from nucleobases to the ligand in its closed conformation. This relationship only deviates in the case of an excitation at 286 nm, which corresponds to the maximal absorbance of N-TASQ. These data imply that the overall increase in fluorescence emission originates from both direct and indirect, quadruplex-mediated excitation of N-TASQ when bound to its target. Similar experiments conducted with ds17 (Figure 2E, and Supporting Information Figure S9) unambiguously show that duplexes cannot elicit the same changes in N-TASQ fluorescent properties (the incoming energy dissipates through radiationless

DOI: 10.1021/jacs.5b03413
J. Am. Chem. Soc. 2015, 137, 8521−8525

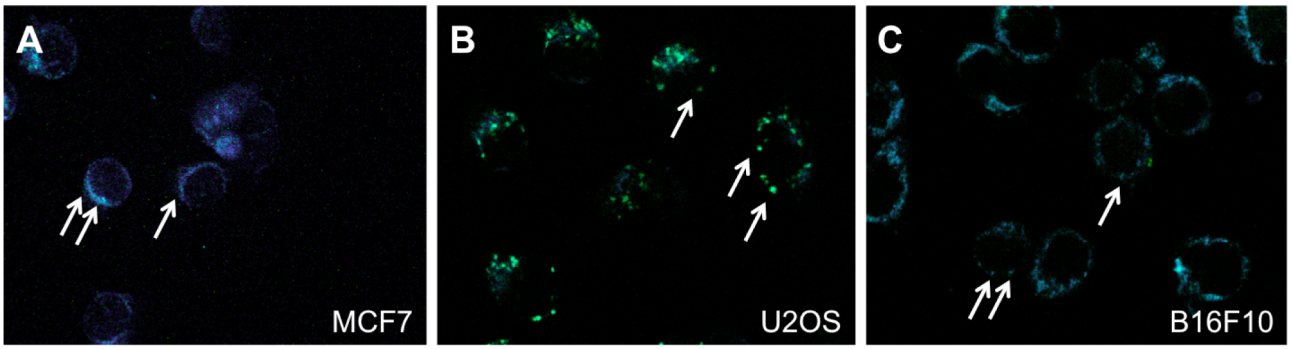

Figure 3. Live-cell imaging of human cells (MCF7 (A) and U2OS (B)) and mouse cells (B16F10 (C)), untreated (i.e., no fixation, permeabilization or mounting steps) but incubated with N-TASQ (5 μM) for 48 h prior to cellular imaging (in phosphate buffer only).

pathways), due to the lack of a nucleic acid-promoted conformational switch. This series of experiments highlight the unique properties of N-TASQ that make it an ideal probe for cellular investigations of quadruplex structures.

We thus tested the ability of N-TASQ to directly detect quadruplexes in cells. Recent reports on quadruplex-specific antibodies have demonstrated their efficiency in the visualization of quadruplexes in human and mouse cells.[8,9] However, antibody-based approaches are limited by (i) the availability of antibodies; (ii) their multistep protocols, involving successive incubations with flag-tagged BG4, antiflag antibodies (either directly conjugated with a fluorophore, or sandwiched with another fluorophore-labeled secondary antibodies), compounded with additional blocking and counterstaining steps; and most importantly (iii) their applications that are restricted to fixed and permeabilized cells. We decided to assess the efficiency of N-TASQ first under identical experimental conditions, to allow for a direct comparison of small-molecule (N-TASQ) versus antibody (BG4) efficiencies. MCF7 cells were prepared according to standard protocols (3.7% paraformaldehyde for fixation, 0.1% Triton X-100 in 1× CSK buffer for permeabilization, hereafter called PFA-triton protocol). After cell fixation, samples were incubated with N-TASQ for 3 h at room temperature. The first multiphoton images were collected after laser excitation at 720 nm, corresponding to the lower limit of the femtosecond laser source (700−1000 nm). High-quality wide-angle fluorescent images were obtained through DAPI (400−492 nm), FITC (500−550 nm) and, to a lesser extent, Alexa emission filters (601−657 nm) (Supporting Information Figure S11). N-TASQ was thus found to be an efficient multiphoton fluorescent probe, labeling foci in the cytoplasmic and nucleolar compartments. However, at this stage, we were not able to conclusively determine the actual N-TASQ *in cellulo* targets in these compartments.

To gain insights into the nature of N-TASQ cellular targets, fixed MCF7 cells were subjected to both DNase and RNase treatments before N-TASQ labeling (Supporting Information Figure S12). While DNase I treatment reduces the difference between cytoplasmic and nuclear staining, RNA digestion induces a notable decrease in total fluorescence, and only the nucleoli remain weakly fluorescent. The nucleoli, which are the site of ribosome synthesis and assembly, comprise tandemly organized GC-rich rDNA (rDNA), RNA (rRNA) and proteins (RNA Polymerase I and RNA modifying enzymes),[25] which make them ideal targets for quadruplex-interacting agents, as demonstrated during the studies of CX-3543.[26] RNase treatment may not have been effective in completely digesting away compacted RNA complexes in the nucleolar compartment. Thus, nucleolar staining, along with the loss of cytoplasmic foci upon RNA digestion, suggests that N-TASQ targets RNA quadruplexes located in the cytoplasm or in the ribosomal machinery.

To further assess this, a series of competitive binding experiments were conducted with N-TASQ and antibodies. We first studied the quadruplex-selective BG4 antibody, which can alternatively stain DNA and RNA quadruplexes depending on the experimental conditions of the immunodetection.[8] We confirmed that fixing conditions were of critical importance (Supporting Information Figures S13 and S14), since BG4 preferentially targets nuclear sites (presumably DNA quadruplexes) after MeOH fixation, and cytoplasmic sites (presumably RNA quadruplexes) after PFA-triton fixation. We used this latter condition as it allows for an efficient BG4/N-TASQ competition for binding to RNA quadruplexes. First, co-incubation with BG4 and N-TASQ results in the loss of cytoplasmic N-TASQ staining (Supporting Information Figure S15), labeling nucleoli only: the observation that BG4 directly competes with N-TASQ for cytoplasmic targets provides another strong argument that N-TASQ targets RNA quadruplexes. Second, we performed an alternative experiment in which MCF7 cells were preincubated with N-TASQ and then postlabeled as above (with both BG4 and N-TASQ). Preincubation allows N-TASQ to interact with quadruplexes before fixation, permeabilization and BG4 incubation steps: the clear multicolor cytoplasmic foci obtained after postlabeling (Supporting Information Figure S16) presumably correspond to ternary N-TASQ/quadruplex/BG4 assemblies, owing to the ability of BG4 to bind to quadruplex/ligand assemblies.[27] This colocalization again strongly implies that N-TASQ targets RNA quadruplexes in cells. Finally, to gain further insights into its cytoplasmic staining pattern, we co-incubated N-TASQ with antibodies raised against calnexin and Rab5, as markers for the endoplasmic reticulum and endosomes, respectively. N-TASQ showed distinct labeling patterns with both antibodies (Supporting Information Figure S17), thereby excluding the possibility that it was confined in these sorting/phagocytotic vesicles. This is in contrast to the BG4 colabeling data that suggested that N-TASQ share common cytoplasmic binding sites (i.e., quadruplexes). These results lend strong support to the assertion that N-TASQ specifically labels RNA quadruplexes in cells.

Finally, we performed quadruplex-labeling experiments directly in live cells, without any cellular treatment (no fixation, permeabilization or mounting steps). Human breast cancer

DOI: 10.1021/jacs.5b03413
J. Am. Chem. Soc. 2015, 137, 8521−8525

(MCF7) and osteosarcoma (U2OS) cell lines, along with murine melanoma (B16F10) cells, were incubated with N-TASQ (5 μM) for 48 h before cellular imaging (in PBS only). Intense and discrete foci were visible exclusively in the cytoplasm of the three cell lines (white arrows, Figure 3 and Supporting Information Figure S18), which might correspond to RNA quadruplexes targeted by N-TASQ either free (in untranslated regions (UTR) of free mRNA)[20] or more likely embedded in more complex subcellular entities (like ribonucleoprotein mRNPs assemblies or granular cytoplasmic P-bodies).[28] Surprisingly, no nuclear foci were observed, suggesting that N-TASQ readily crosses the cytoplasmic membrane but stays within the cytoplasm under physiological (nondenatured) conditions.

CONCLUSION

Discovery of quadruplex-specific antibodies was a milestone in chemical biology. The demonstration that alternative nucleic acid structures exist in cells provides a basis to rethink modern genomics and biology, notably the genetic[1−6] and epigenetic[29] regulatory networks, as well as drug design.[30] Immunofluorescence studies provided solid evidence for the (expected) existence of quadruplexes in the human genome that was greatly expected by the community.[7−10] Our results, which afford an unique, unbiased visualization of quadruplexes in live cells, bring small-molecule detection tools to the forefront of biological investigation of quadruplex cellular functions.[11] Multitasking quadruplex ligands like N-TASQ complement antibody-based cellular detection of quadruplexes, thereby increasing the panoply of molecular tools available for unraveling the biological functions of quadruplexes.

ASSOCIATED CONTENT

Supporting Information

All experimental details and supplementary figures (cited above). The Supporting Information is available free of charge on the ACS Publications website at DOI: 10.1021/jacs.5b03413.

AUTHOR INFORMATION

Corresponding Authors

*jmywong@mail.ubc.ca
*david.monchaud@cnrs.fr

Notes

The authors declare no competing financial interest.

ACKNOWLEDGMENTS

The CNRS, *Université de Bourgogne* (uB), and *Conseil Régional de Bourgogne* (CRB) are acknowledged for funding (3MIM project). Prof. Shankar Balasubramanian (Cambridge University, U.K.) is warmly thanked for the generous gift of BG4 plasmid and Prof. Jerry Pelletier (McGill University, Canada) for insightful discussions.

REFERENCES

(1) Murat, P.; Balasubramanian, S. *Curr. Opin. Gen. Dev.* **2014**, *25*, 22.
(2) Collie, G. W.; Parkinson, G. N. *Chem. Soc. Rev.* **2011**, *40*, 5867.
(3) (a) Yang, D.; Okamoto, K. *Future Med. Chem.* **2010**, *2*, 619. (b) Phan, A. T. *FEBS J.* **2010**, *277*, 1107.
(4) Maizels, N.; Gray, L. T. *PLoS Genet.* **2013**, *9*, e1003468.
(5) (a) Bochman, M. L.; Paeschke, K.; Zakian, V. A. *Nat. Rev. Genet.* **2012**, *13*, 770. (b) Tarsounas, M.; Tijsterman, M. *J. Mol. Biol.* **2013**, *425*, 4782.
(6) Oganesian, L.; Karlseder, J. *J. Cell Sci.* **2009**, *122*, 4013.
(7) (a) Schaffitzel, C.; Berger, I.; Postberg, J.; Hanes, J.; Lipps, H. J.; Pluckthun, A. *Proc. Natl. Acad. Sci. U.S.A.* **2001**, *98*, 8572. (b) Schaffitzel, C.; Postberg, J.; Paeschke, K.; Lipps, H. J. *Methods Mol. Biol.* **2010**, *608*, 159.
(8) (a) Biffi, G.; Tannahill, D.; McCafferty, J.; Balasubramanian, S. *Nat. Chem.* **2013**, *5*, 182. (b) Biffi, G.; Di Antonio, M.; Tannahill, D.; Balasubramanian, S. *Nat. Chem.* **2014**, *6*, 75.
(9) Henderson, A.; Wu, Y.; Huang, Y. C.; Chavez, E. A.; Platt, J.; Johnson, F. B.; Brosh, R. M., Jr.; Sen, D.; Lansdrop, P. M. *Nucleic Acids Res.* **2014**, *42*, 860.
(10) (a) Rodriguez, R.; Miller, K. M.; Forment, J. V.; Bradshaw, C. R.; Nikan, M.; Britton, S.; Oelschlaegel, T.; Xhemalce, B.; Balasubramanian, S.; Jackson, S. P. *Nat. Chem. Biol.* **2012**, *8*, 301. (b) Di Antonio, M.; Rodriguez, R.; Balasubramanian, S. *Methods* **2012**, *57*, 84.
(11) (a) Largy, E.; Granzhan, A.; Hamon, F.; Verga, D.; Teulade-Fichou, M.-P. *Top. Curr. Chem.* **2012**, *330*, 111. (b) Vummidi, B. R.; Alzeer, J.; Luedtke, N. W. *ChemBioChem* **2013**, *14*, 540. (c) Bhasikuttan, A. C.; Mohanty, J. *Chem. Commun.* **2015**, *51*, 7581.
(12) (a) Chang, C.-C.; Chu, J.-F.; Kao, F.-J.; Chiu, Y.-C.; Lou, P.-J.; Chen, H.-C.; Chang, T.-C. *Anal. Chem.* **2006**, *78*, 2810. (b) Tseng, T.-Y.; Chien, C.-H.; Chu, J.-F.; Huang, W.-C.; Lin, M.-Y.; Chang, C.-C.; Chang, T.-C. *J. Biomed. Opt.* **2013**, *18*, 101309.
(13) (a) Stefan, L.; Guédin, A.; Amrane, S.; Smith, N.; Denat, F.; Mergny, J.-L.; Monchaud, D. *Chem. Commun.* **2011**, *47*, 4992. (b) Stefan, L.; Denat, F.; Monchaud, D. *J. Am. Chem. Soc.* **2011**, *133*, 20405.
(14) (a) Haudecoeur, R.; Stefan, L.; Denat, F.; Monchaud, D. *J. Am. Chem. Soc.* **2013**, *135*, 550. (b) Haudecoeur, R.; Stefan, L.; Monchaud, D. *Chem.—Eur. J.* **2013**, *19*, 12739.
(15) Laguerre, A.; Stefan, L.; Larrouy, M.; Genest, D.; Novotna, J.; Pirrotta, M.; Monchaud, D. *J. Am. Chem. Soc.* **2014**, *136*, 12406.
(16) (a) Cassar, L. *J. Organomet. Chem.* **1975**, *93*, 253. (b) Dieck, H. A.; Heck, F. R. *J. Organomet. Chem.* **1975**, *93*, 259. (c) Sonogashira, K.; Tohda, Y.; Hagihara, N. *Tetrahedron Lett.* **1975**, 4467. (d) Doucet, H.; Hierso, J.-C. *Angew. Chem., Int. Ed.* **2007**, *46*, 834.
(17) Shinamura, S.; Osaka, I.; Miyazaki, E.; Nakao, A.; Yamagishi, M.; Takeya, J.; Takimiya, K. *J. Am. Chem. Soc.* **2011**, *133*, 5024.
(18) Renciuk, D.; Zhou, J.; Beaurepaire, L.; Guédin, A.; Bourdoncle, A.; Mergny, J.-L. *Methods* **2012**, *57*, 122.
(19) Balasubramanian, S.; Hurley, L. H.; Neidle, S. *Nat. Rev. Drug Discovery* **2011**, *10*, 261.
(20) Bugaut, A.; Balasubramanian, S. *Nucleic Acids Res.* **2012**, *40*, 472719.
(21) (a) Anders, A. *Opt. Commun.* **1978**, *26*, 339. (b) Anders, A. *Appl. Phys.* **1979**, *18*, 333.
(22) (a) Lubitz, I.; Borovok, N.; Kotlyar, A. *Biochem.* **2007**, *46*, 12925. (b) Kong, D.-M.; Ma, Y.-E.; Wu, J.; Shen, H.-X. *Chem.—Eur. J.* **2009**, *15*, 901.
(23) Foncesca Guerra, C.; Zijlstra, H.; Paragi, G.; Bickelhaupt, F. M. *Chem.—Eur. J.* **2011**, *17*, 12612.
(24) Karsisotis, A. I.; Hessari, N. M.; Novellino, E.; Spada, G. P.; Randazzo, A.; Webba da Silva, M. *Angew. Chem., Int. Ed.* **2011**, *50*, 10645.
(25) Boisvert, F.-M.; van Koningsbruggen, S.; Navascues, J.; Lamond, A. I. *Nat. Rev. Mol. Cell Biol.* **2007**, *8*, 574.
(26) Drygin, D.; Siddiqui-Jain, A.; O'Brien, S.; Schwaebe, M.; Lin, A.; Bliesath, J.; Ho, C. B.; Proffitt, C.; Trent, K.; Whitten, J. P.; Lim, J. K. C.; Von Hoff, D.; Anderes, K.; Rice, W. G. *Cancer Res.* **2009**, *69*, 7653.
(27) Yangyuoru, P. M.; Di Antonio, M.; Ghimire, C.; Biffi, G.; Balasubramanian, S.; Mao, H. *Angew. Chem., Int. Ed.* **2015**, *54*, 910.
(28) (a) Eulalio, A.; Behm-Ansmant, I.; Izaurralde, E. *Nat. Rev. Mol. Cell Biol.* **2007**, *8*, 9. (b) Parker, R.; Sheth, U. *Mol. Cell Rev.* **2007**, *25*, 635.
(29) De, S.; Michor, F. *Nat. Struct. Mol. Biol.* **2011**, *18*, 950.
(30) Rodriguez, R.; Miller, K. M. *Nat. Rev. Genet.* **2014**, *15*, 783.

DOI: 10.1021/jacs.5b03413
J. Am. Chem. Soc. 2015, 137, 8521−8525